CONF-9510189--5

LA-UR- 95-3432

Title: SATBOT I: PROTOTYPE OF A BIOMORPHIC AUTONOMOUS SPACECRAFT

Author(s): Janette Frigo
Mark W. Tilden

Submitted to: SPIE

Los Alamos
NATIONAL LABORATORY

Form No. 836 R5
ST 2629 10/91

SATBOT I: prototype of a biomorphic autonomous spacecraft

Janette Frigo and Mark W. Tilden
Los Alamos National Laboratory, NIS-1
Los Alamos, New Mexico 87545

ABSTRACT

Our goal is to produce a prototype of an autonomous satellite robot, SATBOT. This robot differs from conventional robots in that it has three degrees of freedom, uses magnetics to direct the motion, and needs a zero gravity environment. The design integrates the robot's structure and a biomorphic (biological morphology) control system to produce a survival-oriented vehicle that adapts to an unknown environment. Biomorphic systems, loosely modeled after biological systems, use simple analog circuitry, low power, and are microprocessor independent. These analog networks called Nervous Networks (Nv), are used to solve real-time controls problems. The Nv approach to problem solving in the robotics has produced many surprisingly capable machines which exhibit emergent behavior.[1] The network can be designed to respond to positive or negative inputs from a sensor and produce a desired directed motion. The fluidity and direction of motion is set by the neurons and is inherent to the structure of the device. The robot is designed to orient itself with respect to a local magnetic field; to direct its attitude toward the greatest source of light; and robustly recover from variations in the local magnetic field, power source, or structural stability. This design uses a two neuron network which acts as a push-pull controller for the actuator (air core coil), and two sun sensors (photodiodes) as bias inputs to the neuron. The effect of sensor activation as it relates to an attractive or repulsive torque (directional motion) is studied. A discussion of this system's power (energy) efficiency and frequency, noise immunity, and some dynamic characteristics is presented.

1. INTRODUCTION

Most spacecraft developed for scientific, communications, navigation, and military uses are custom designed for the requirements of the payload. This process costs millions of dollars and takes years of development. Furthermore, the investment is jeopardized by subsystem failures, particularly in the control system.

A space environment demands that the control system be low power, robust, reliable, and autonomous while being able to withstand severe temperature, shock, vibration, and radiation-hardness levels. Over the past fifty years there have been dramatic improvements in methods of designing spacecraft systems; however, every conceivable failure-mode cannot be predicted. Control systems must adapt to failures. For example, the Department of Energy's (DOE) ALEXIS spacecraft experienced structural damage during launch which caused orientation problems and loss of subsequent communications for part of the mission. The ALEXIS control system has not functioned autonomously after this failure. Currently, all control operations for ALEXIS are sent up from the ground.

Satellite systems of the future, for example Iridium, a constellation of 66 satellites used for global communications, require more efficient, reliable, and autonomous systems. In this paper we investigate an analog neural network controller that locates the autonomy of the control system in the hardware, aims to control the vehicle attitude (motion) for survival, to seek the greatest source of sunlight, and robustly responds to variations in the magnetic field, power, etc. To accomplish this task, a series of prototype robots, SATBOT I, were developed to test the control methodology. We analyze the performance of two prototypes, SATBOT 1.3 and 1.4, by

calculating the magnetic torque acting on the vehicle and compare them with other magnetic torque controlled spacecraft.

2. NERVOUS NETWORKS

Much of control systems and systems theory is derived from mathematics such as Lyapunov's Stability Theory. Our approach differs in that it is motivated by biological neurons/nervous systems. Many neural systems in nature are surprisingly adaptive and efficient. Taking advantage of the solutions nature provides, researchers such as Hopfield[2] are building analog models of specific nervous system functions.

An explanation of the elementary function of artificial neurons is useful for the development of the Nv neuron model. The human nervous system is an analog system which consists of approximately ten trillion neurons,[3] each having the ability to receive, process, and transmit electrochemical signals over complex pathways. Neurons are connected by dendrites which extend from cell body to cell body. Signals are received at a connection point called synapse and sent to the cell body. The inputs are summed. The input either excites or inhibits the cell. If the cumulative excitation in the cell body exceeds a threshold, the cell fires, sending the signal to the other neurons. The Nv neuron and most artificial neural networks model these simple neuron characteristics.

2.1 Central Pattern Generators (CPGs)

Oscillatory neural networks are groups of neurons responsible for a wide variety of periodic behavior patterns such as locomotion, breathing, and chewing. The study of oscillatory neural networks in invertebrates accounts for much of what is known about this rhythmic behavior. Documented examples include the digestive rhythms of the lobster, stepping movements of the cockroach, and the rapid wing motion of the locust during flight.[4] In general, these types of networks are capable of generating oscillatory activity without requiring some sensory input, although some do require a form of initial excitation.[5] Such networks are referred to as central pattern generators.

How do CPGs work? Neuronal oscillators could work in two ways: (1) one or more cells embedded in a network have the property of bursting (cell-driven oscillators) or (2) the network itself produces bursts as a result of synaptic interactions. Several combinations of such networks exist. A hybrid form in which the oscillatory pattern is generated by both bursty cells and network interactions (mixed oscillators) is the predominant form.[5] These networks consist mainly of inhibitory synapses.

Some CPGs are capable of producing multiple patterns of activity. The small, localized CPGs which occur in invertebrates make it possible to study the relationship between the emergent collective behavior of the biological network and the network's underlying circuitry. Much has been done to analyze the dynamical properties of invertebrate CPGs. Cellular, synaptic, and connectivity properties have been experimentally manipulated. Cell interactions within the network have been simulated and analytical equations describing the network dynamics have been developed.[4] There is no precise explanation for the mechanisms that control frequency, duration, and phase relations of the motor pattern. Studies of invertebrate CPGs such as Getting's network simulation of the escape swimming rhythm of the mollusc[4] show that the generation of these rhythms is a complicated process involving the influence of multiple modulators which modify the output of the circuit.

The architectures (or topologies) of connectionists models for artificial neural networks are not biologically realistic. Neurons have complex physiological properties that are important to their

computation and time dependent properties that are ignored in most models. An exception is a computational model in which the sizes of variables are represented by the explicit times at which action potential (neuronal firing) occurs.[2] Analog information is represented by using the timing of action potentials with respect to a continuous collective oscillatory pattern. Experiments on rat hippocampal 'place cells' and electric fish show this action-potential phase-time coding.[2]

2.2 Nv network model

The mechanisms that control frequency, duration, and phase relations of the motor pattern of a CPG do not have a precise explanation. The mechanisms by which Nv networks function are similarly illusive, as shown by the dynamics of motion of a variety of walking robots that solve complex problems and exhibit emergent behavior.[1] The nervous network does not attempt to approximate a particular mechanism, but instead achieves a dynamical solution via a unique implementation of the neuron. The architecture of the network, the frequency, and the phase relationship between neurons in the network are an integral part of the dynamical solution.

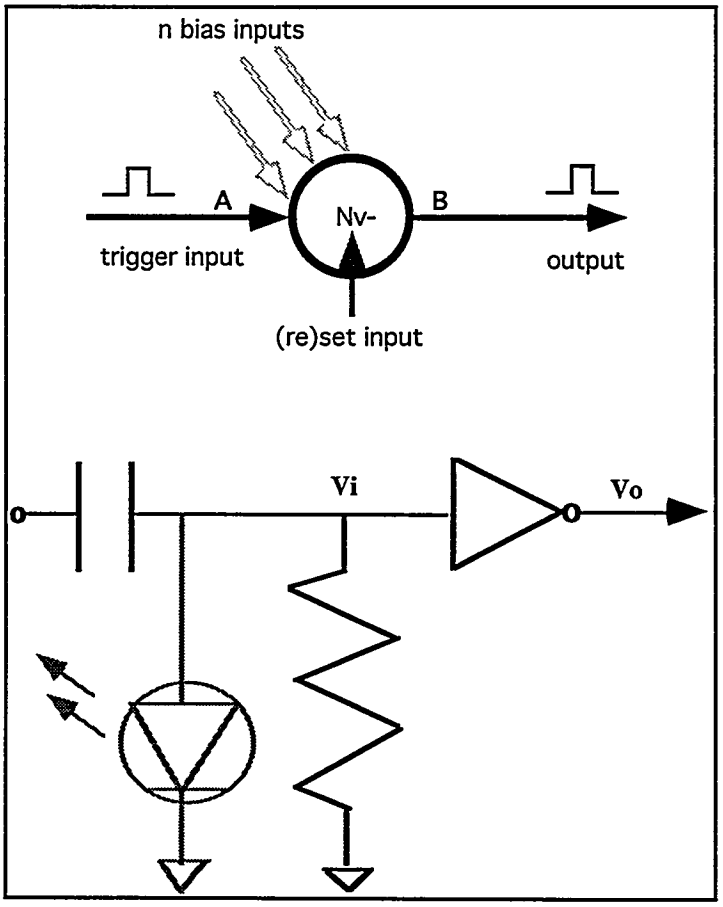

Fig. 1. The Nv motor neuron symbol (top) and schematic(bottom). (Nv-) denotes negative edge triggered. The SATBOT I systems use this neuron configuration.

The Nv neuron is an digital summing differentiator neuron which determines the triggering and time delay of signals (or processes) through the network. Fig. 1 contains the symbol for the Nv

motor neuron. Like the artificial neuron, the input delay to the neuron is set by the sum of the external bias inputs. In this case, it is a high pass delay. Based on the inner threshold level, the output changes state. The schematic in Fig. 1 shows an inhibitory neuron. The inverting buffer-driver (a Schmidt trigger) is a comparator with hysteresis. The input delay is modulated via sensor activation which decreases the time constant of the neuron and the power across the output load.

The Nv network is a directed loop of two or more neurons. Different architectures associated with these multiple neuron circuits and their respective phase spaces are shown in Fig. 2.

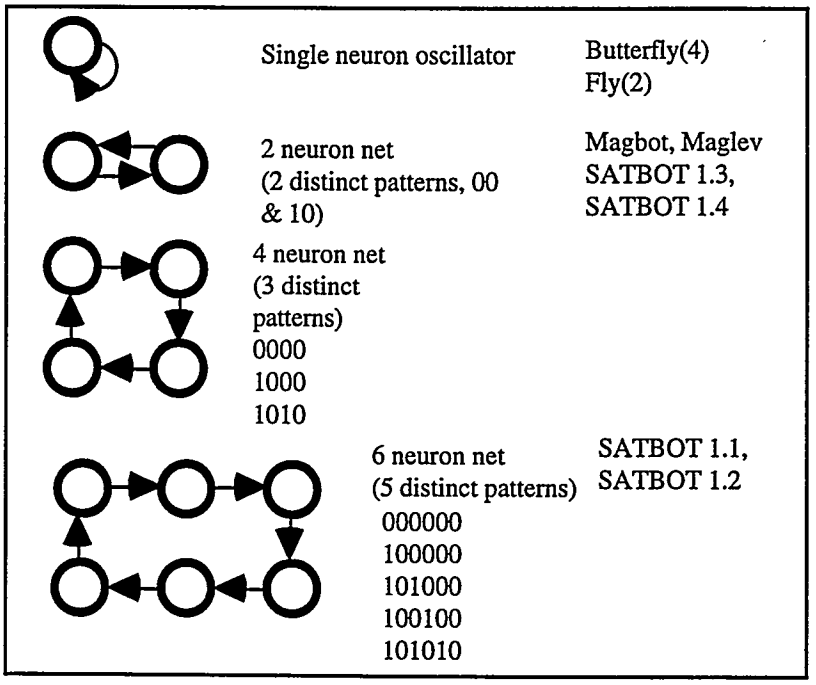

Fig. 2. Topological structure of Nv control systems.

3. BIOMORPHIC CONTROL SYSTEMS

Biomorphic control (from the Greek word biology "to live" and morphology "to take form") systems place an equal importance on mechanical and electrical structure. The structures are an integral part of one another and a deficiency in either hierarchy yields a less successful, less capable device. A biomorphic, autonomous system attempts to (1) achieve directed motion in the environment, (2) procure abundant power, and (3) robustly (even aggressively) negotiate obstacles.[1]

The autonomy of these robots is inherent to their structure. The robot has no knowledge of the surrounding environment and its motion is not controlled by a microprocessor. Rather, an analog computation of the sensory input and the internal process state produces a directed response. The tenuous relationship between weight to power, mass imbalances, coupling and biasing the neuron for dynamic motion are the challenges of designing a biomorhpic system.

The research completed includes 12 different robots which use magnetic torque coils for actuation. The design method for a single neuron, a six neuron, and a two neuron system is presented. A discussion of the performance objectives concludes this section.

3.1 Single neuron magnetic thruster prototypes

A schematic for the basic two transistor circuit called the Nv solarengine is shown in Fig. 3. The idea was to develop a single neuron device that was capable of directed motion with respect to a magnetic field and study the power verse frequency characteristics of the neuron.

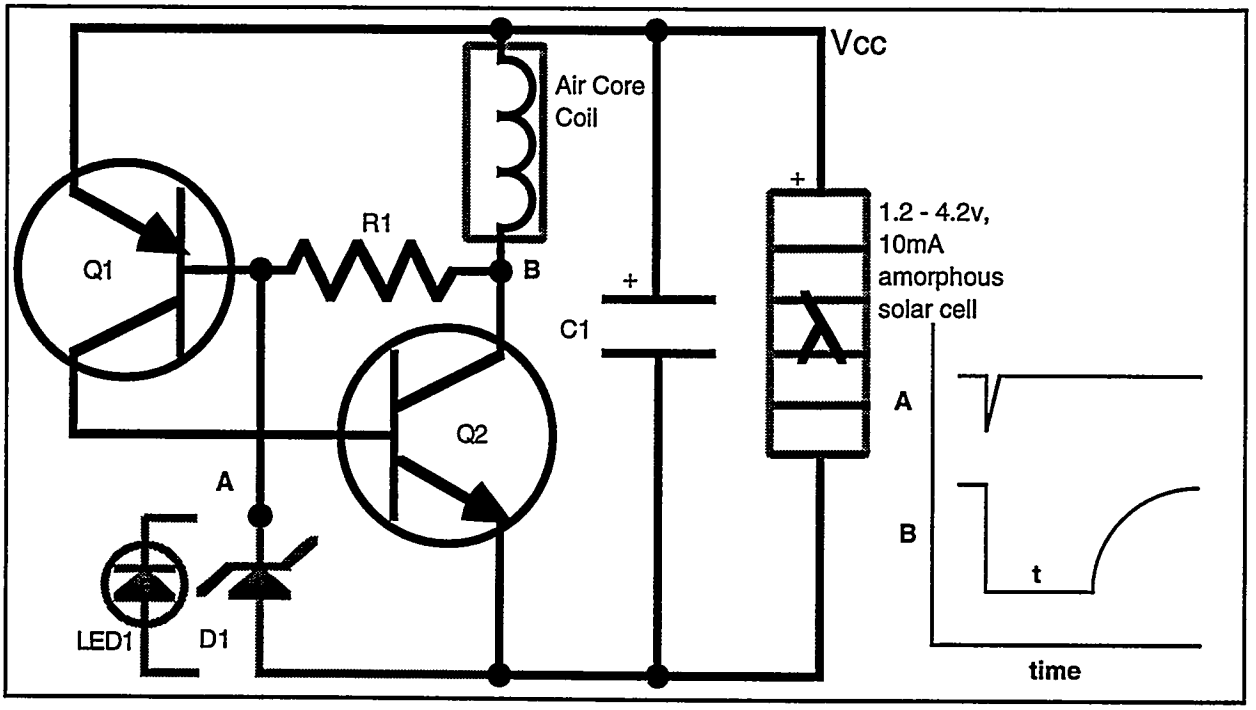

Fig. 3. The Solarengine* schematic (Nv-). *Solarengine (Pat. #5,3225,031) is a modified silicon control rectifier with supercritical feedback.

The solar cell charges the capacitor, C1. As voltage increases, the LED1 begins to conduct, building up a 0.7v drop (with respect to Vcc) which turns on transistor, Q1. Transistor Q1 in turn triggers Q2 into a low impedance or "on" state (turning on the motor) as long as charge remains in the capacitor, C1. When the capacitor looses charge, the transistors turn off and the process starts again. These robots (Butterfly, Fly in Fig. 2) are called "magnetic thrusters" since current is pulsed through the coil in one direction. The circuit can operate on voltages as low as 1.2 volts.

What is the power verses frequency characteristic of this neuron? In direct light, the capacitor stores maximum charge, and the circuit triggers at a higher frequency. Maximum current applied to the actuators yields a maximum torque. In dim light a slower frequency produces less torque. As the circuit reaches maximum power, the frequency approaches resonance. Neurons implemented in subsequent designs use different discrete components (Fig. 1), but continuously operate variable frequency and power.

3.2 Six neuron push-pull prototypes

For larger Nv loops more actuators can be used with a greater number of process states. Two prototypes in Fig. 2 use a six neuron network and three coils mounted along the x/y/z axes. One coil is connected across the outputs of two neurons, therefore, the direction of current changes as each neuron pulses. The two neurons are a push-pull pair with respect to one actuator (coil). Fig. 4 below shows the input/output relationship for such a neuron pair. The sensors are photodiodes coupled directly to the input bias. See Fig. 1. The devices are suspended above from a string. The

magnetic field used is a ceramic, cylindrical magnet with a measured axial component of 100 Gauss (approximately one inch from the surface).

The sensory activation did not yield significant directional motion for this design. The weight (49.6 g) to power (0.40 watts) ratio was too great, and the device had insufficient force. In general, the suspension method was cumbersome and could not show the dynamic range of the device. Our redesign objectives were to modify the sensor bias input, minimize the weight of the device, and improve the suspension method.

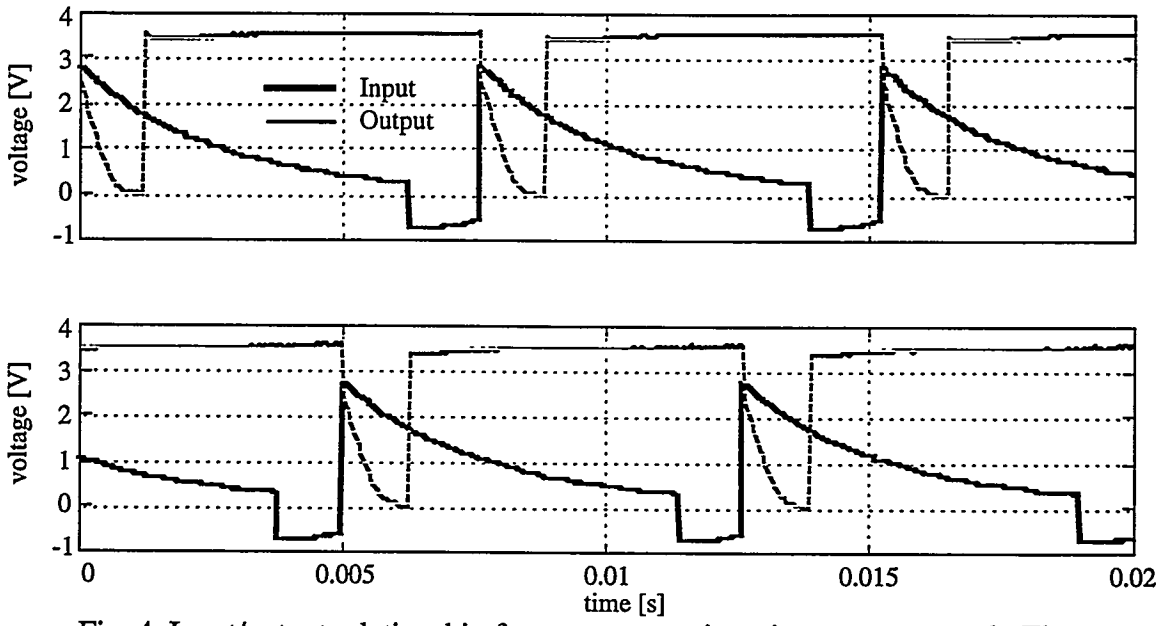

Fig. 4. Input/output relationship for two neurons in a six neuron network. The neurons are spaced 120° apart.

3.3 Implementation of two neuron push-pull prototypes

The most successful designs, SATBOT 1.3, 1.4, use a two neuron network and push-pull actuation with respect to a single coil. The circuit configuration in Fig. 5 is called a bicore.

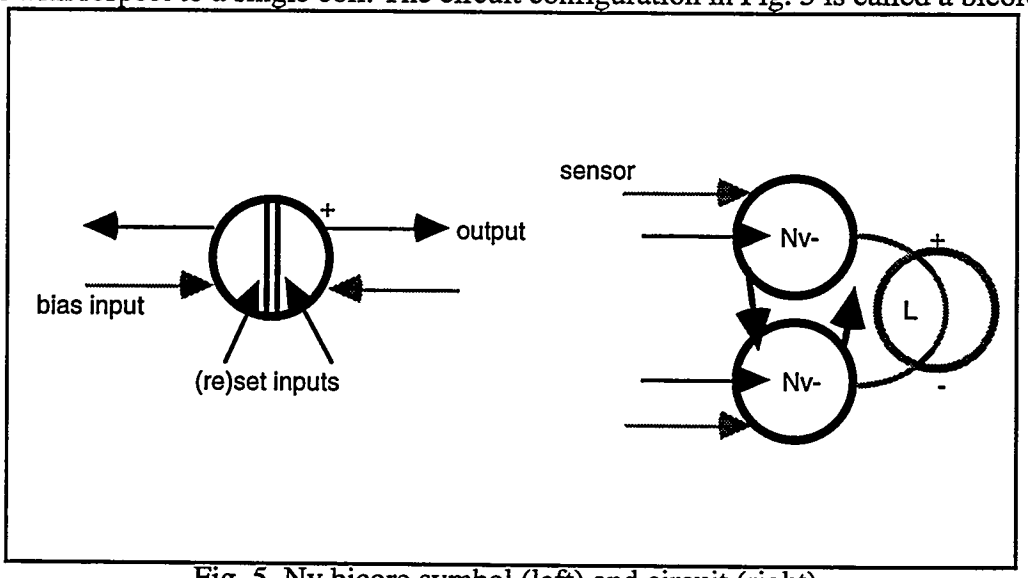

Fig. 5. Nv bicore symbol (left) and circuit (right).

3.3.1 Mechanical structure

How does this design achieve an improved weight verses power ratio? The structure consists of one coil connected across the outputs of two neurons. The power supply is a single solar cell and two charge capacitors. The neurons are implemented with one integrated circuit, using two photodiodes as two sun sensors. See Table 1. The magnetic field used is a ceramic, cylindrical magnet with measured axial component of 100 Gauss (approximately one inch from the surface). The center of mass on the structure was determined and a pin was mounted from beneath to suspend the device. The weight is balanced by adding a blast at a distance from the center of mass, balancing each axis. The force acting on the actuator is in the opposite direction of the thrust, therefore, it is important to have the structure well balanced.

3.3.2 Neuron bias

Next, the sensor placement, and input biases were determined. The sensor location was determined by finding the focal point at which the field of view for each sensor overlaps. There is a solution where equal activation of the sensors at this focal point yields stability. The neurons are inhibitory (Fig. 1). This means the sensor when activated will decrease the time constant of the neuron and with respect to the neuron pair, one frequency is increased. This difference causes more power in the opposite direction of sensor activation, and a torque in the direction of the light source. The activation can be varied, but as long as one sensor is activated more than the other, the motion will be directed toward the sensor with greatest activation. In the same way, the sensors could be reversed to cause motion away from the light if desired. Hence, the robot knows nothing of what direction it is supposed to move, rather, the designer has chosen to bias the neuron to cause motion toward the light source. After many iterations a bias value is found that is commensurate with a predetermined velocity.

3.3.3 Discussion - performance

The system performance shows the responsiveness of our robots to the local magnetic field. This field was chosen for connivance in demonstrating the principle concept. We observed the prototype, SATBOT 1.4, track the greatest source of light in its rotational axis and recover from variations in the magnetic field, power source or the moment of inertia (due to structural damage). Table 1 below is a summary of the mechanical, electrical and dynamic characteristics of SATBOT 1.4.

Table 1. SATBOT 1.4 characteristics.

Mechanical/Dynamic	Components	Electrical
Weight: 20.84 grams	74HCT240	Power: 5.6v, 35ma
Torque: 10e-06* n-m	one solar cell	Frequency: 37.8 Hz
Magnetic Flux: 100*G	two photodiodes	Neurons: two Nv
*experimental measurement	inductor: 500mH	
	resistors, capacitors	

4. RESULTS

A discussion of the power/energy efficiency and noise immunity shows some advantages of the Nv network especially for an exoatmospheric environment. A brief summary of magnetic stabilization control is given, and the magnetic control torque, etc. for our system is compared to some magnetic torque controlled spacecraft missions.

4.1 Power verse frequency

The period for one, two, and three process states is represented as follows:

$$\tau_1 = \sum_{i=1}^{6} R_i C \quad , \qquad \tau_2 = \sum_{i=1}^{2} R_i C \quad , \qquad \tau_3 = R_1 C \tag{1}$$

where the value of capacitance, C, is consistent across the network and i = 1, 2,...., 6 represent the smallest to the largest values of resistance, R_i. At saturation, $\tau_3 = R_1 C$, the frequency is the greatest. Energy across the inductive load is:

$$E(t) = \frac{1}{2} L i(t)^2 \text{ joules} \tag{2}$$

$$i(t) = i(t_o) + \frac{1}{L} \int_{t_o}^{t} v(x)dx \tag{3}$$

where i(t), is the expression for current in an inductor.

The input/output voltage for a balanced (all RC time constants are equal) six neuron network with three process states are shown in Fig. 6. The network was chosen to illustrate the power /frequency relationship of Nv networks. The frequencies for the one process, two process, and saturation state are 75 Hz, 227 Hz, and 454 Hz respectively. The input is an exponential decay set by the bias input, which turns on the neuron output within a certain input voltage threshold. This threshold, approximately 2.7 to 1.8 volts for the one process state (Fig. 1), determines the output response of the neuron, and the amount of time current is delivered to the load. Fig. 7 shows the output response of a two neuron push-pull pair for this network and the corresponding inductor load voltage. This one process state has a energy/period ratio of 0.41 joules. A trigger, or state transition is introduced to the input of a neuron which causes two signals to propagate around the network (two process state). As shown below in Fig. 6 and eqn. (1) the frequency increases and the energy/period is decreased to 0.04 joules. The three process state has a energy ratio of 0.15 joules. We expect the second process state to have a higher energy/period ratio than the saturation state, however, in this circuit the two process state reaches a highly reactive state, almost a 50/50 duty cycle due to the saturation of the supply voltage. In general, the power or energy consumption is less for increasing process states.

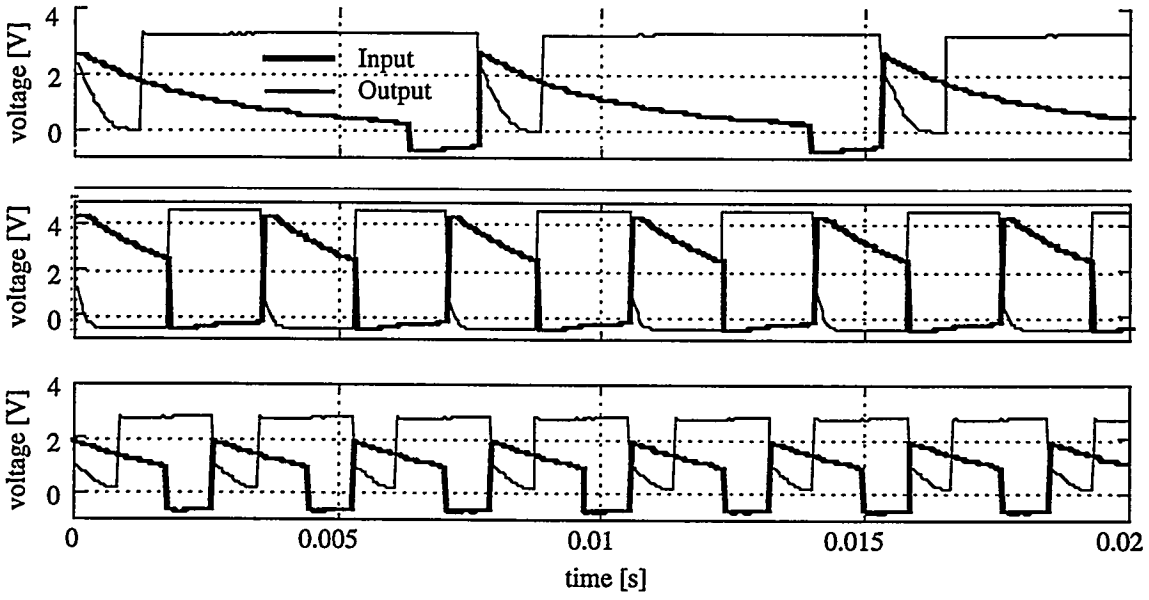

Fig. 6. Process states of a six Nv network. The input voltage and output response(top to bottom) for the one process, two process, and saturation states are shown.

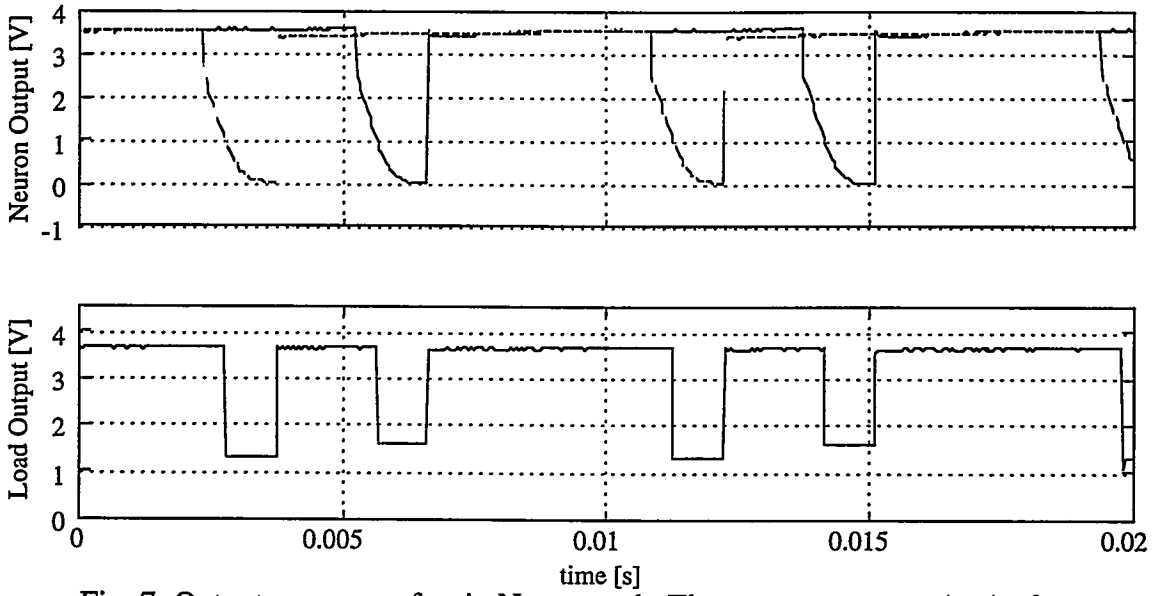

Fig. 7. Output response of a six Nv network. The output response (top) of two neurons spaced 120° apart. The voltage output (bottom) across the load (inductor). This is the one process state at a frequency of 75 Hz.

The PSpice simulation shows the results of an unbalanced six neuron network with a transformer load connected across the output of a neuron pair. The frequency of the network is 72 Hz for a one process state. The output response in Fig. 8 (top) across the inductive load shows the expected inrush current spike when the neuron turns on and off. The experimental data shows similar characteristics Fig. 7 if measurements are taken with finer resolution. The input/output characteristics of the neuron pair (bottom) match the experimental values from above. (The two neurons have a time constant of 2.4 ms and 1.7 ms respectively compared to the experimental data which is 2.2 ms).

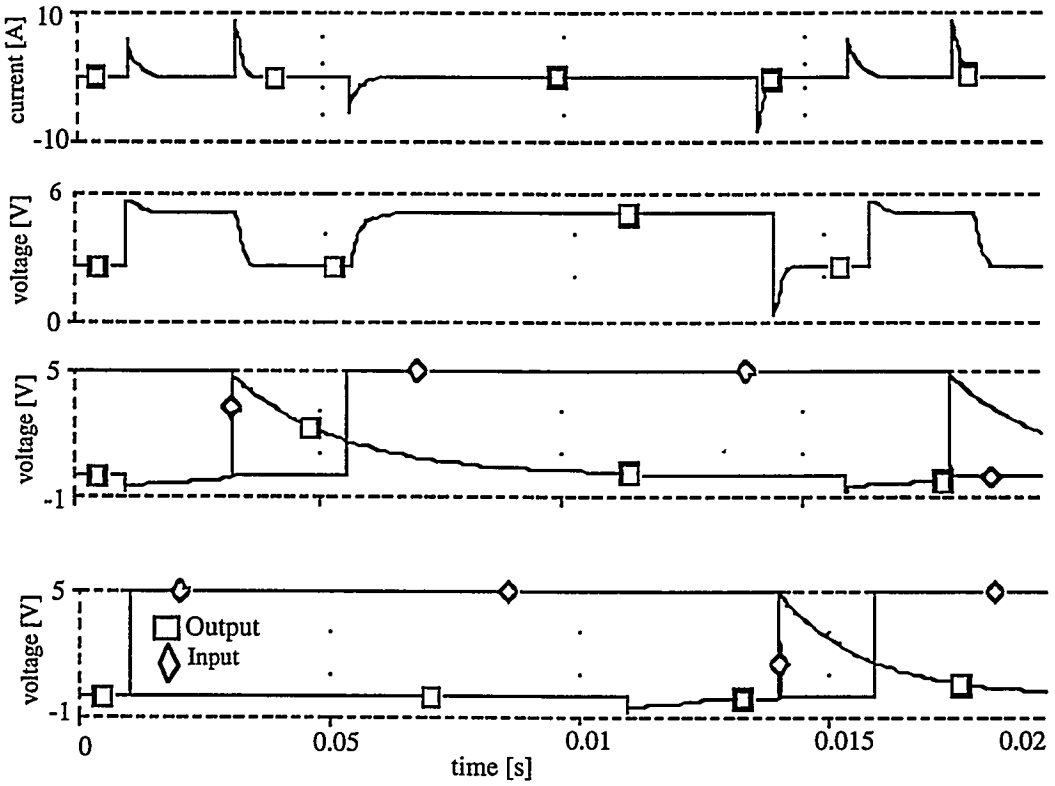

Fig. 8. PSpice simulation for an unbalanced six neuron network with an inductive load. The inductor current and voltage characteristics (top) and the input/output voltages (bottom) for a two neuron push-pull pair is shown. One neuron has a $\tau = RC = 2.4$ ms (third plot from the top) and the other has $\tau = RC = 1.7$ ms (bottom). The neurons have a 120° phase space.

4.2 Noise immunity

The network tends to have a high noise immunity. The Nv neuron is a comparator with hysteresis Fig. 9. There is a hysteresis width V2 - V1, of input voltages for which the output will not change state. The output responds mainly to large variations in the sign of the derivative of the input. Small changes in the input cause almost no change in the output due to the exponential decay of the response. Sudden spikes, changing the input sign, do not disrupt the output if they are instantaneous and the voltage across the capacitor has not caught up with the input voltage before the spike disappears[6] Nv systems have motor loads and inductive loads causing back emf and noise on the source voltage, but they operate nominally despite the noise on the power supply. This is an advantage for spacecraft avionics as electomagnetic interference (EMI) testing is a required qualification test. The network has a set process/frequency space, and a noise signal may change the process state of the network. If an appropriate delay is introduced to terminate additional processes, and return the network to its original state, the noise is rejected.

4.3 Torque considerations - magnetic stabilization

The objective for an attitude control system is to reorient the spacecraft from one attitude to another. The Earth's magnetic field and magnetic coils are used to control direction and/or spin maneuvers in space. Magnetic stabilization methods use combinations of magnetic torquers, dual-spin, momentum bias, reaction wheels, and control moment gyro systems.[7] In this case, a simplified example of the system will suffice.

The magnetic torque **T** acting on a satellite in orbit is the vector cross-product of the spacecraft magnetic dipole moment **M** and the local magnetic induction or flux density **B**. The equation in vector notation is

$$\mathbf{T} = \mathbf{M} \times \mathbf{B}, \quad \text{n-m} \tag{4}$$

where the magnetic moment, **M**, of an electromagnet aligned with the spin axis (spin axis coil) is

$$\mathbf{M} = m_o u \hat{s}, \quad \text{A-m}^2 \qquad -1 < u < 1 \tag{5}$$

$$m_o = INA\hat{s} \tag{6}$$

$$d = \mu m_o \hat{s}, \quad \text{W} \cdot \text{m} \tag{7}$$

where $\hat{s} \equiv w$ is a unit vector along the spin axis; The maximum magnetic moment is m_o and N is the number of turns for a coil, A is the enclosed area of the current loop, and I is the current through the loop. The commendable coil state parameter, u, is proportional to the current through the coil and is either positive or negative depending on the direction of current flow clockwise or counterclockwise relative to s. The maximum dipole moment is d, where μ is the permeability of the core material. The time rate of change of angular momentum is equal to the total torque on the spacecraft,

$$\mathbf{T} = \frac{d\mathbf{H}}{dt} = H\frac{d\hat{s}}{dt} \tag{8}$$

$$H = \hat{i}I_{xx}w_x + \hat{j}I_{yy}w_y + \hat{k}I_{zz}w_z, \quad kg \cdot m^2 / s \tag{9}$$

In eqn. (4) **M** is parallel with **s**, thus, the torque is also orthogonal to H, the angular momentum (the magnitude of H remains constant). In this case, the angular momentum is the moment of inertia at the principle axis of inertia, I, times the angular velocity, w.

Eqn. (4) through (9) were used to calculate torque for the SATBOT 1.3 and 1.4 prototypes. The results are shown below in Table 2 and compared to some other spacecraft structures.

Table 2. Characteristics of Spin Axis Magnetic Coils on Spacecraft Missions.[8]

Spacecraft	Angular Momentum $kg \cdot m^2 / s$	Maximum Dipole $W \cdot m$	Magnetic Torque *flux at 10e-05T *n-m*	Power *watts*
SAS-3	4.465	6.28e-5	–	10W, 0.6 amps, 260 turns
OSO-8	342.6	5.33e-5	–	0.075 amps, 360 turns
SATBOT 1.3		6.20e-10	4.94e-09*	0.2W, 0.035 amps, 200 turns
SATBOT 1.4	5.70e-08*	2.20e-10	1.75e-09*	0.2W, 0.035amps, 100 turns

5. CONCLUSION

We designed a functional prototype which can stabilize its position with respect to a local magnetic field and rotate toward the greatest source of light. The system can adapt to variations in the magnetic field, power source, or the structure. The efficiency and power vs. frequency were discussed since the system can operate in different states as an emergent function of the network and as shown the energy dissipated at these higher frequencies decreases. The noise immunity of the system is due to the fundamental structure of the neuron, a hysteresis differentiator. These characteristics are all advantages in a space environment. Lastly, the dynamic characteristics of this system suggests sufficient torque and power characteristics given the simple model we have constructed.

7. REFERENCES

[1] Hasslacher, B., and Tilden, Mark W., "Living Machines," Robotics and Autonomous System: The Biology and Technology of Intelligent Autonomous Agents, Elsivier Publishers, Spring 1995.

[2] Hopfield, J. J., "Pattern recognition computing using action potential timing for stimulus representation," Vol. 376, pp. 33-36, 1995.

[3] Wasserman, Philip D., "*Neural Computing Theory and Practice*," Chp. 1-2, Van Hostrand Reinhold, New York, 1989.

[4] Bower, James M. and Beeman, David, *The Book of GENESIS*, Chp. 8, TELOS, Santa Clara, 1995.

[5] Selverston, Allen I. and Moulins, Maurice, "Oscillatory Nerual Networks", *Vol. 47*, pp. 29-48, Annual Reviews, Inc., 1985.

[6] Mead, C., *Analog VLSI and Neural Systems*, Chp. 10, Addison-Wesley Publishing Company, Inc., New York, 1989.

[7] Chobotov, V. A., *Spacecraft Attitude Dynamics and Control*, Chp. 8, Krieger Publishing Co., Malabar, 1991.

[8] Wertz, James R., *Spacecraft Attitude Determination and Control*, Chp. 6 and 19, Kluwer Academic Publishers, Dordrecht, 1978.